JACC: CARDIOVASCULAR IMAGING VOL. 5, NO. 9, 2012

ISSN 1936-878X/$36.00

PUBLISHED BY ELSEVIER INC.

http://dx.doi.org/10.1016/j.jcmg.2012.02.016

Effects of p38 Mitogen-Activated Protein Kinase Inhibition on Vascular and Systemic Inflammation in Patients With Atherosclerosis

Maysoon Elkhawad, MBBCHIR, MA,*† James H. F. Rudd, MBCHB, PHD,†
Lea Sarov-Blat, PHD,‡ Gengqian Cai, PHD,‡ Richard Wells, BA,*
L. Ceri Davies, MD, MBBS,§ David J. Collier, PHD, MBBS,§
Michael S. Marber, MBBS, PHD,‖ Robin P. Choudhury, BMBCH, MA, DM,¶
Zahi A. Fayad, PHD,# Ahmed Tawakol, MD,** Fergus V. Gleeson, MBBS,¶
John J. Lepore, MD,‡ Bill Davis, PHD,†† Robert N. Willette, PHD,‡
Ian B. Wilkinson, BMBCH, DM,* Dennis L. Sprecher, MD,‡ Joseph Cheriyan, MBCHB*†‡‡‡

Cambridge, London, and Oxford, United Kingdom; King of Prussia, Pennsylvania; New York, New York; and Boston, Massachusetts

OBJECTIVES This study sought to determine the effects of a p38 mitogen-activated protein kinase inhibitor, losmapimod, on vascular inflammation, by ^{18}F-fluorodeoxyglucose (FDG) positron emission tomography/computed tomography imaging.

BACKGROUND The p38 mitogen-activated protein kinase cascade plays an important role in the initiation and progression of inflammatory diseases, including atherosclerosis.

METHODS Patients with atherosclerosis on stable statin therapy (n = 99) were randomized to receive losmapimod 7.5 mg once daily (lower dose [LD]), twice daily (higher dose [HD]) or placebo for 84 days. Vascular inflammation was assessed by FDG positron emission tomography/computed tomography imaging of the carotid arteries and aorta; analyses focused on the index vessel (the artery with the highest average maximum tissue-to-background ratio [TBR] at baseline). Serum inflammatory biomarkers and FDG uptake in visceral and subcutaneous fat were also measured.

RESULTS The primary endpoint, change from baseline in average TBR across all segments in the index vessel, was not significantly different between HD and placebo (ΔTBR: −0.04 [95% confidence interval [CI]: −0.14 to +0.06], p = 0.452) or LD and placebo (ΔTBR: −0.02 [95% CI: −0.11 to +0.06], p = 0.579). However, there was a statistically significant reduction in average TBR in active segments (TBR ≥1.6) (HD vs. placebo: ΔTBR: −0.10 [95% CI: −0.19 to −0.02], p = 0.0125; LD vs. placebo: ΔTBR: −0.10 [95% CI: −0.18 to −0.02], p = 0.0194). The probability of a segment being active was also significantly reduced for HD when compared with placebo (OR: 0.57 [95% CI: 0.41 to 0.81], p = 0.002). Within the HD group, reductions were observed in placebo-corrected inflammatory biomarkers including high-sensitivity C-reactive protein (% reduction: −28% [95% CI: −46 to −5], p = 0.023) as well as FDG uptake in visceral fat (ΔSUV: −0.05 [95% CI: −0.09 to −0.01], p = 0.018), but not subcutaneous fat.

CONCLUSIONS Despite nonsignificant changes for the primary endpoint of average vessel TBR, HD losmapimod reduced vascular inflammation in the most inflamed regions, concurrent with a reduction in inflammatory biomarkers and FDG uptake in visceral fat. These results suggest a systemic anti-inflammatory effect. (A Study to Evaluate the Effects of 3 Months Dosing With GW856553, as Assessed FDG-PET/CT Imaging; NCT00633022) (J Am Coll Cardiol Img 2012;5:911–22) © 2012 by the American College of Cardiology Foundation

From the *Clinical Pharmacology Unit, University of Cambridge, Cambridge, United Kingdom; †Division of Cardiovascular Medicine, University of Cambridge, Cambridge, United Kingdom; ‡Metabolic Pathways & Cardiovascular Therapy Area Unit,

Atherosclerosis is considered to be a complex, chronic, progressive inflammatory condition (1), involving cytokines that direct the adhesion and transmigration of monocytes into the vascular wall. This complex process requires the modulation of a number of cell signaling pathways in which p38 mitogen-activated protein kinases (MAPK) play a fundamental role (2,3). Four p38 MAPK isoforms have been identified, with the alpha and beta isotypes being prominent in the heart and vasculature, and delta and lambda isotypes in skeletal muscle, lung, and renal tissues. The expression and activity of p38 MAPKs are relatively low in healthy vasculature yet markedly elevated in macrophages of atherosclerotic lesions (2).

In pre-clinical models of cardiovascular disease, p38 MAPK inhibition improves endothelial dysfunction, limits atherogenesis, and improves survival (4,5). Additionally, p38 MAPK inhibition reduces macrophage-associated plaque inflammation in apolipoprotein E–deficient mice, assessed using magnetic resonance imaging (6). We have previously demonstrated that p38 MAPK inhibition attenuates release of high-sensitivity C-reactive protein (hsCRP) in patients undergoing angioplasty (7), and, using a potent and specific alpha/beta p38 MAPK inhibitor, losmapimod (5), improves vasoregulation in hypercholesterolemic patients (8), supporting translation of pre-clinical results into humans.

Cellular ^{18}F-fluorodeoxyglucose (FDG) uptake, measured by positron emission tomography/computed tomography (PET/CT), correlates with macrophage glucose consumption (9), macrophage number (10,11), and is also influenced by the degree of hypoxia (12) in atherosclerosis, all potential markers of plaque vulnerability. FDG-PET/CT imaging has been successfully used to determine culprit plaques responsible for transient ischemic attack and stroke (13). In addition, FDG uptake is attenuated by statins, with reductions in FDG uptake observed in both animal and human models of atherosclerosis (10,14). Although FDG-PET/CT has not been validated for predicting cardiovascular events, it may serve to answer mechanistic questions about macrophage-focused effects on vascular inflammation when assessing novel anti-inflammatory compounds (13–16).

ABBREVIATIONS AND ACRONYMS

CI = confidence interval
FDG = fluorodeoxyglucose
HD = higher dose
hsCRP = high-sensitivity C-reactive protein
LD = lower dose
MAPK = mitogen-activated protein kinase
PET/CT = positron emission tomography/computed tomography
SUV = standard uptake value
TBR = tissue-to-background ratio

In this exploratory study, the primary objective was to test the hypothesis that selective p38 MAPK

GlaxoSmithKline, King of Prussia, Pennsylvania; §Centre of Clinical Pharmacology, William Harvey Research Institute, Bart's and The London School of Medicine and Dentistry, Queen Mary University of London, London, United Kingdom; ‖King's College, London, United Kingdom; ¶University of Oxford, Oxford, United Kingdom; #Mount Sinai Medical Centre, New York, New York; **Massachusetts General Hospital and Harvard Medical School, Boston, Massachusetts; ††GlaxoSmithKline Clinical Unit, Cambridge, United Kingdom; and the ‡‡Cambridge University Hospitals National Health Service Foundation Trust, Cambridge, United Kingdom. This study was funded by GlaxoSmithKline. Ms. Elkhawad, and Drs. Rudd, Wilkinson, and Cheriyan, as well as the Cambridge University Hospitals PET/CT Unit, have received funding support from National Institute for Health Research (NIHR) Cambridge Comprehensive Biomedical Research Centre. Ms. Elkhawad has received funding support from the Raymond and Beverly Sackler Foundation. Drs. Rudd and Wilkinson are consultants for GlaxoSmithKline. Drs. Sarov-Blat, Cai, Lepore, Davis, Willette, and Sprecher are employees of and own stock in GlaxoSmithKline. Mr. Wells has reported that he has no relationships relevant to the contents of this paper to disclose. Drs. Davies and Collier have received funding from NIHR Cardiovascular Biomedical Research Unit, Bart's and the London School of Medicine and Dentistry. Dr. Collier has received a research grant from GlaxoSmithKline for this study. Dr. Marber has received funding from the NIHR Comprehensive Biomedical Research Centre, Guy's and St Thomas's National Health Service Foundation Trust in partnership with the British Heart Foundation Centre, King's College, London. He has received a research grant from and is a consultant for GlaxoSmithKline for this compound. Drs. Choudhury and Gleeson have received funding from the NIHR Oxford Comprehensive Biomedical Research Centre. Dr. Choudhury is a Wellcome Trust Senior Research fellow and is supported by the British Heart Foundation Centre for Research Excellence, Oxford. He has received a research grant for this study and is on the advisory board of AstraZeneca and Roche. Dr. Fayad has received research grants from GlaxoSmithKline, AstraZeneca, Roche, Bristol-Myers Squibb Merck & Co. Inc., VBL Therapeutics, Philips, Siemens, Novartis, and the National Institute of Health. Dr. Tawakol has received research grants from Bristol-Myers Squibb, GlaxoSmithKline, Merck & Co. Inc., Genentech/Roche, VBL Therapeutics, Siemens, Novartis, and the National Institute of Health. He consults for Bristol-Myers Squibb, GlaxoSmithKline, Merck & Co. Inc., Novartis, and Roche. Dr. Wilkinson has received funding support from the British Heart Foundation as a funded post holder; he has also received educational grants from GlaxoSmithKline for current clinical trials. Dr. Cheriyan is employed by Cambridge University Hospitals National Health Service Foundation Trust and is obligated to spend 50% of his time on GlaxoSmithKline clinical trial research, representing a significant relationship; however, he receives no other benefits or compensations from GlaxoSmithKline. Ms. Elkhawad and Dr. Rudd contributed equally to this paper. H. William Strauss, MD, served as Guest Editor for this paper.

Manuscript received September 10, 2011; revised manuscript received January 13, 2012, accepted February 29, 2012.

inhibition with losmapimod reduces vascular inflammation (as assessed with FDG-PET/CT imaging) in stable atherosclerotic patients on concurrent statin therapy. Pre-specified secondary objectives included safety, tolerability, and effects on serum inflammatory biomarkers. Finally, to determine effects on extravascular inflammation, FDG uptake in visceral and subcutaneous fat was also measured. Visceral fat is relevant to the metabolic risk associated with cardiovascular disease (17,18).

METHODS

Study design. This was a phase II, randomized, double-blind, placebo-controlled study conducted at 4 sites in the United Kingdom (Cambridge University Hospitals National Health Service Foundation Trust; Bart's and The London School of Medicine and Dentistry; University of Oxford; and King's Health Partners, London). The protocol was approved by Oxfordshire Research Ethics Committee and registered with ClinicalTrials.gov (NCT00633022). The study complied with the Declaration of Helsinki and written informed consent was obtained from all participants.

Study population. Patients age 50 to 80 years with a history of atherosclerosis (clinically stable, at least 6 months after myocardial infarction, transient ischemic attack/stroke, or symptomatic peripheral vascular disease) and with a body mass index between 19 and 35 kg/m^2 were eligible. Patients were on stable statin therapy. Prior to enrolment, eligible patients underwent a screening PET/CT to determine whether they had sufficient vascular inflammation for study entry, defined as an average arterial FDG whole vessel tissue-to-background ratio (TBR) of ≥1.6 (11) in either of the carotids or the ascending aorta. Patients with New York Heart Association functional class II to IV heart failure, atrial fibrillation, hepatic or renal disease, poorly controlled type II diabetes, insulin-dependent diabetics, and those with chronic inflammatory conditions and malignancy were excluded.

Intervention. Patients were randomized (1:1:1) to receive oral losmapimod 7.5 mg twice daily (higher dose [HD]), losmapimod 7.5 mg once daily (lower dose [LD]), or placebo for 84 days. Losmapimod and placebo tablets were indistinguishable and study personnel and patients were blinded to treatment allocation until the trial was complete. Study medication was manufactured by GlaxoSmithKline.

Vascular and fat PET/CT imaging. Vascular PET/CT imaging (19,20) was performed at study entry (pre-dose) and repeated at day 84. Vessels were identified and sectioned into 5-mm contiguous "segments." Regions of interest were drawn around the arterial wall (in the axial plane) for every segment of the coregistered PET/CT images. The maximum standard uptake value (SUV) of FDG in each segment was recorded and normalized to background blood FDG activity, yielding a TBR. For each patient, the artery with the highest average maximum TBR at baseline was designated the "index vessel" (either carotid artery or aorta) and was used for further analyses. The index vessels were evaluated using a "whole vessel" approach and an "active segment" approach (Fig. 1). With the whole vessel approach, all segments composing the index vessel were analyzed, regardless of whether or not active inflammation was present at baseline. In the active segment approach, noninflamed segments were excluded, similar to previous work in which the effect of simvastatin was assessed only in locations with increased FDG uptake at baseline (14,21). Prior FDG-PET imaging studies with pathological correlations demonstrate that a TBR value <1.6 is associated with <5% inflammation within the atheroma (11,22–24). Therefore, segments with TBR ≥1.6 were defined as active. Measurements of visceral and subcutaneous fat were performed as previously described (25). See the supplementary methods in the Online Appendix for additional details.

Laboratory assessments. Blood samples were collected pre-dose on days 1, 7, 14, 28, 56, and 84 and 2 weeks post-cessation of drug for measurement of hsCRP and pre-dose on days 1, 28 or 42, and 84 for measurement of inflammatory biomarkers. All analyses were conducted centrally using standard laboratory methods.

Safety assessments. Adverse events, safety laboratory parameters, hemodynamic variables, and electrocardiograms were assessed throughout the study.

Statistical methods. A sample size of 30 patients per group provided 90% power to detect a 15% difference in change from baseline in TBR across all segments within the index vessel with a 5% level of significance (14).

The safety population included patients who received at least 1 dose of the investigational product. Change from baseline analyses for pharmacodynamics and FDG-PET/CT included patients with both baseline and post-baseline values.

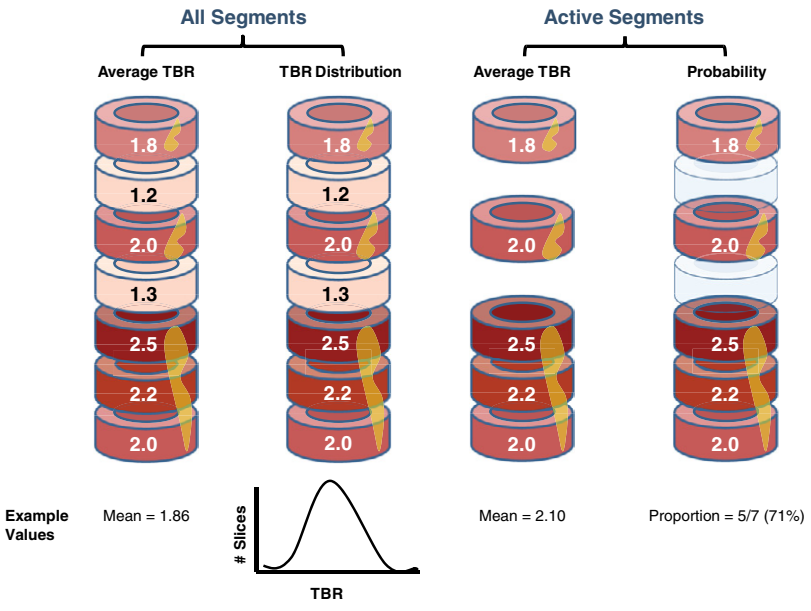

Figure 1. Analysis Methods Used To Quantify Vascular Inflammation in the Index Vessel

A series of contiguous segments from the index vessel are illustrated. Atherosclerotic plaques in the vessel wall are indicated in **yellow.** The value within each segment represents the maximum tissue-to-background ratio (TBR) for that segment. Active segments were pre-defined as segments with TBR ≥1.6.

We used 3 approaches to quantify vascular inflammation (Fig. 1): 1) the pre-specified whole vessel primary endpoint of change in the average maximum TBR for all segments within the index vessel (19), with a complementary post hoc analysis displaying the group distribution of TBR using a frequency histogram; 2) an analysis of change from baseline in average maximum TBR for active seg-

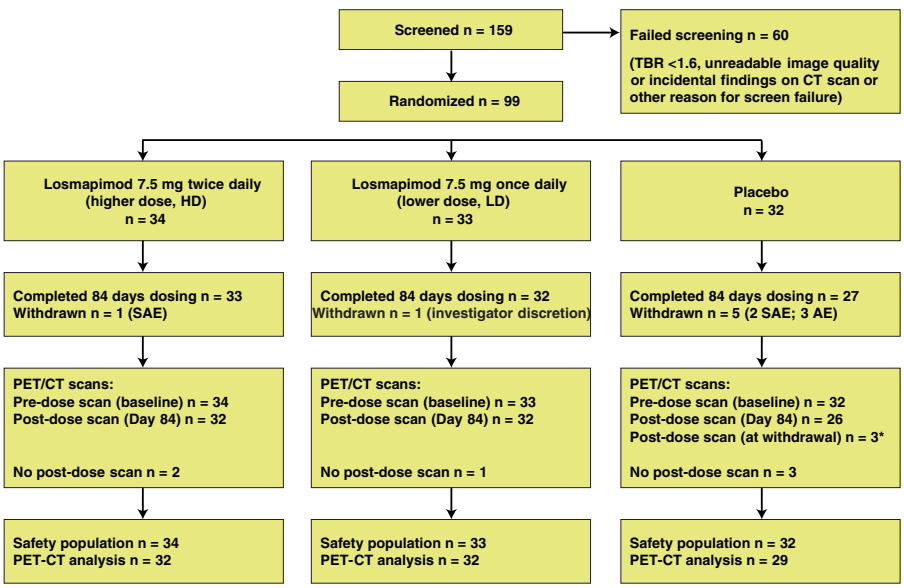

Figure 2. Flow of Patients Through the Trial

*Patients who withdrew after receiving ≥2 months of treatment had a post-dose positron emission tomography/computed tomography (PET/CT) scan at the time of withdrawal. These patients are included in the PET/CT analysis. AE = adverse event; HD = higher dose; LD = lower dose; SAE = serious adverse event; TBR = tissue-to-background ratio.

ments within the index vessel; and 3) an analysis of the probability of a segment being active within the index vessel.

Change from baseline in average maximum TBR was analyzed using analysis of covariance, fitting treatment as fixed effect, and including baseline value as a covariate. Point estimates and corresponding 95% confidence intervals (CI) were constructed for the relevant comparisons of interest.

TBR data were plotted to show the distribution from all segments from all index vessels within each treatment group (at pre-dose and post-dose). The Kolmogorov-Smirnov statistic was applied to these data to measure the effect of treatment on TBR distribution. The difference between losmapimod and placebo was calculated and tested using a nonparametric permutation test at the patient level. Baseline correction is not feasible with this analysis approach.

The number of active segments and the total number of segments were included in logistic regression analyses to model the probability of a segment being active. For baseline correction within each group, a model was fitted with terms for treatment and day. For placebo and baseline correction, a model was fitted with treatment term and including the baseline proportion of active segments as covariate. In the baseline correction within each group model, the generalized estimating equation method was used to adjust for the fact that multiple

Table 1. Demographic and Baseline Characteristics

		Losmapimod		
	Placebo (n = 32)	LD (n = 33)	HD (n = 34)	Total (n = 99)
Demographics				
Male/female	28/4	28/5	29/5	85/14
Age, yrs	63.7 ± 6.37	65.3 ± 5.94	62.3 ± 5.90	63.8 ± 6.01
Body mass index, kg/m^2	28.9 ± 3.44	28.0 ± 3.35	29.8 ± 3.68	28.9 ± 3.46
Medical history				
Current or ex-smoker	22 (69)	22 (67)	27 (79)	71 (72)
Acute coronary syndrome or myocardial infarction	17 (53)	18 (55)	22 (65)	57 (58)
Transient ischemic attack/stroke	4 (13)	10 (30)	10 (29)	24 (24)
Peripheral vascular disease	5 (16)	3 (9)	4 (12)	12 (12)
Type 2 diabetes mellitus	3 (9)	1 (3)	2 (6)	6 (6)
Concomitant medications*				
Antiplatelet therapies	28 (88)	30 (91)	29 (85)	87 (88)
ACEI or ARB	22 (69)	24 (73)	26 (76)	72(73)
Beta-blockers	18 (56)	15 (45)	22 (65)	55 (56)
Other antihypertensives	15 (47)	10 (30)	14 (41)	39 (39)
Oral hypoglycemics	2 (6)	0	3 (9)	5 (5)
Baseline values†				
Systolic blood pressure, mm Hg	130 (19)	133 (16)	135 (17)	133 (17)
Diastolic blood pressure, mm Hg	76 (8)	77 (11)	79 (9)	77 (9)
Glucose, mmol/l	5.81 (1.02)	5.74 (0.60)	5.99 (1.05)	5.85 (0.90)
Glucose, mg/dl	104.60 (18.41)	103.30 (10.82)	107.80 (18.83)	105.30 (16.27)
Cholesterol, mmol/l	4.20 (0.88)	3.91 (0.75)	3.71 (0.74)	3.78 (0.94)
Cholesterol, mg/dl	150.97 (49.64)	144.24 (28.76)	143.24 (28.65)	146.07 (36.41)
HDL cholesterol, mmol/l	1.23 (0.28)	1.23 (0.32)	1.16 (0.30)	1.20 (0.30)
HDL cholesterol, mg/dl	47.49 (10.66)	47.49 (12.39)	44.79 (11.97)	46.56 (11.59)
LDL cholesterol, mmol/l	2.22 (0.67)	2.01 (0.51)	1.91 (0.61)*	2.05 (0.59)
LDL cholesterol, mg/dl	85.71 (25.79)	77.61 (19.85)	74.32 (23.63)*	79.10 (22.96)
Triglycerides, mmol/l	1.63 (0.56)	1.46 (0.74)	1.40 (0.51)	1.49 (0.60)
Triglycerides, mg/dl	144.25 (49.65)	129.20 (65.66)	123.89 (45.04)	132.24 (53.58)
hsCRP, mg/l‡	1.00 (133)	1.30 (146)	1.30 (114)	1.20 (122)
Adiponectin, ng/ml†	11,219 (31)	10,932 (45)	10,110 (37)	10,732 (38)

Values are mean ± SD or n (%). *All patients were on statins for at least 3 months before the study. †hsCRP and adiponectin are reported as geometric mean (% coefficient of variation). ‡hsCRP values >10 mg/l were omitted.

ACEI = angiotensin-converting enzyme inhibitor; ARB = angiotensin receptor blocker; HD = higher dose (losmapimod 7.5 mg twice daily); HDL = high-density lipoprotein; hsCRP = high-sensitivity C-reactive protein; LD = lower dose (losmapimod 7.5 mg once daily); LDL = low-density lipoprotein.

data points (day 1 and day 84) were from the same vessel (patient). Point estimates and corresponding 95% CI were constructed to establish the odds ratio for the relevant comparisons of interest.

Biomarker data were analyzed by analysis of covariance fitting terms for regimen, day, and interaction of day and regimen as fixed effects; patient as a random effect; and baseline biomarker at day 1 as a covariate.

Statistical analyses were performed using SAS version 9.2 (SAS Institute, Cary, North Carolina). No multiplicity adjustment was made and p values <0.05 were considered statistically significant.

RESULTS

The flow of participants through the study is shown in Figure 2: 159 patients were screened; 99 were randomized; 92 completed the 84-day dosing period; and 93 were included in FDG-PET/CT analyses. Demographic and baseline characteristics are summarized in Table 1. A summary of index vessel types for each group is shown in Online Table 1.

Vascular PET/CT imaging. ALL SEGMENTS. Figure 3 illustrates the patchy nature of vascular inflammation in atherosclerosis. The magnitude of reduction in average maximum TBR of all segments within the index vessel was larger in the losmapimod groups, but there was no significant difference when compared with placebo (Table 2). There was, however, a significant leftward shift in TBR distribution from baseline to day 84 in the losmapimod groups (HD vs. placebo: p = 0.007; LD vs. placebo: p = 0.031), with no significant change in the placebo group (Fig. 4).

ACTIVE SEGMENTS. When only active segments were considered, there was a statistically significant reduction in average maximum TBR in these in-

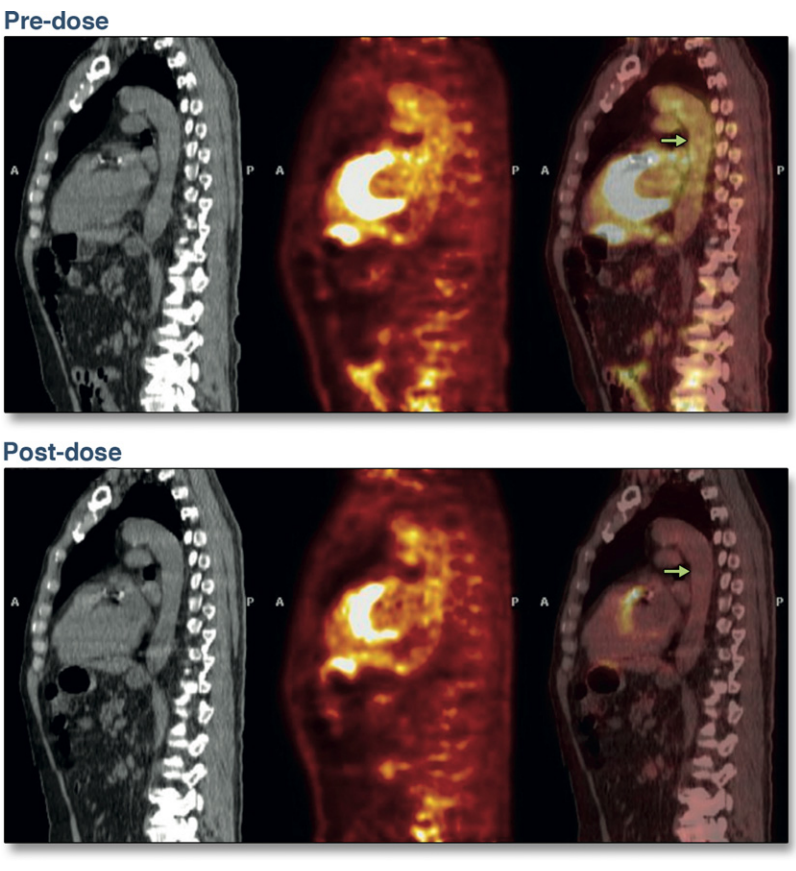

Figure 3. Typical FDG-PET/CT Images

(A) From left to right, sagittal CT, PET, and combined CT and PET images from a patient at pre-dose (baseline) are shown. **(B)** Matching images from the same patient after 84 days of treatment with losmapimod HD. The **arrows** highlight the descending aorta, demonstrating heterogeneous atherosclerotic fluorine ^{18}F-fluorodeoxyglucose (FDG) uptake, which is lowered post-dose. Other abbreviations as in Figure 2.

Table 2. Change from Baseline in FDG Uptake in the Index Vessel

Change From Baseline in Average Maximum TBR for All Segments Within the Index Vessel

	Mean ± SD TBR		Day 84 Versus Baseline*			Placebo and Baseline Corrected*		
Group	Baseline	Day 84	Difference	95% CI	p Value	Difference	95% CI	p Value
HD, n = 32	2.07 ± 0.31	1.93 ± 0.30	−0.13	−0.21 to −0.05	0.003	−0.04	−0.14 to 0.06	0.452
LD, n = 32	2.05 ± 0.22	1.93 ± 0.20	−0.12	−0.17 to −0.06	<0.001	−0.02	−0.11 to 0.06	0.579
Placebo, n = 29	1.94 ± 0.24	1.89 ± 0.25	−0.09	−0.16 to −0.03	0.005	NA	NA	NA

Change From Baseline in Average Maximum TBR for Active Segments (Segments With Maximum TBR ≥1.6)

	Mean ± SD TBR		Day 84 Versus Baseline*			Placebo and Baseline Corrected*		
Group	Baseline	Day 84	Difference	95% CI	p Value	Difference	95% CI	p Value
HD, n = 32	2.03 ± 0.30	1.86 ± 0.27	−0.14	−0.20 to −0.08	<0.001	−0.10	−0.19 to −0.02	0.013
LD, n = 32	2.03 ± 0.22	1.87 ± 0.19	−0.14	−0.20 to −0.07	<0.001	−0.10	−0.18 to −0.02	0.019
Placebo, n = 29	1.86 ± 0.20	1.84 ± 0.20	−0.04	−0.09 to 0.02	0.177	NA	NA	NA

Change From Baseline in Probability of a Segment Being Active (TBR ≥1.6)

	% of Active Segments ± SD		Day 84 Versus Baseline†			Placebo and Baseline Corrected†		
Group	Baseline	Day 84	Odds Ratio	95% CI	p Value	Odds Ratio	95% CI	p Value
HD, n = 32	94.4% ± 9.4	84.6% ± 21.3	0.19	0.08 to 0.47	<0.001	0.57	0.41 to 0.81	0.002
LD, n = 32	95.3% ± 8.2	89.1% ± 19.7	0.39	0.22 to 0.69	0.001	1.17	0.80 to 1.71	0.429
Placebo, n = 29	88.3% ± 19.2	82.2% ± 24.4	0.90	0.50 to 1.62	0.736	NA	NA	NA

*Difference, 95% CI, and p value for comparison derived from analysis of covariance. †Odds ratio, 95% CI, and p value for comparison derived from logistic regression analyses on odds ratio scale. Day 84 versus baseline result is from the model of baseline correction within each group; placebo and baseline corrected result is from the model with both placebo and baseline correction.
CI = confidence interval; FDG = fluorodeoxyglucose; NA = not applicable; TBR, tissue-to-background ratio; other abbreviations as in Table 1.

flamed areas for both HD and LD losmapimod compared with placebo (p = 0.0125 and p = 0.0194, respectively) (Table 2).

The odds of having an active segment on day 84 was significantly lower than on day 1 for the HD group (p < 0.001) and the LD group (p = 0.001),

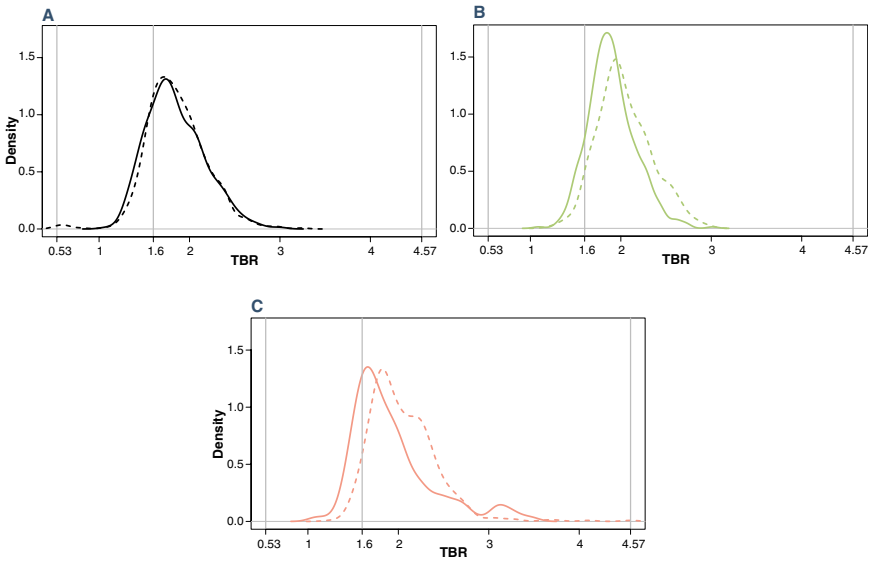

Figure 4. Frequency Histograms of All Segments From the Index Vessel

Frequency histograms of all segments from the index vessel histograms show tissue-to-background ratio (TBR) data from all patients in the placebo group **(A)** at pre-dose baseline **(black dashed line)** and after 84 days **(black solid line),** in the losmapimod LD group **(B)** at pre-dose baseline **(green dashed line)** and after 84 days **(green solid line),** and in the losmapimod HD group **(C)** at pre-dose baseline **(pink dashed line)** and after 84 days **(pink solid line)**.

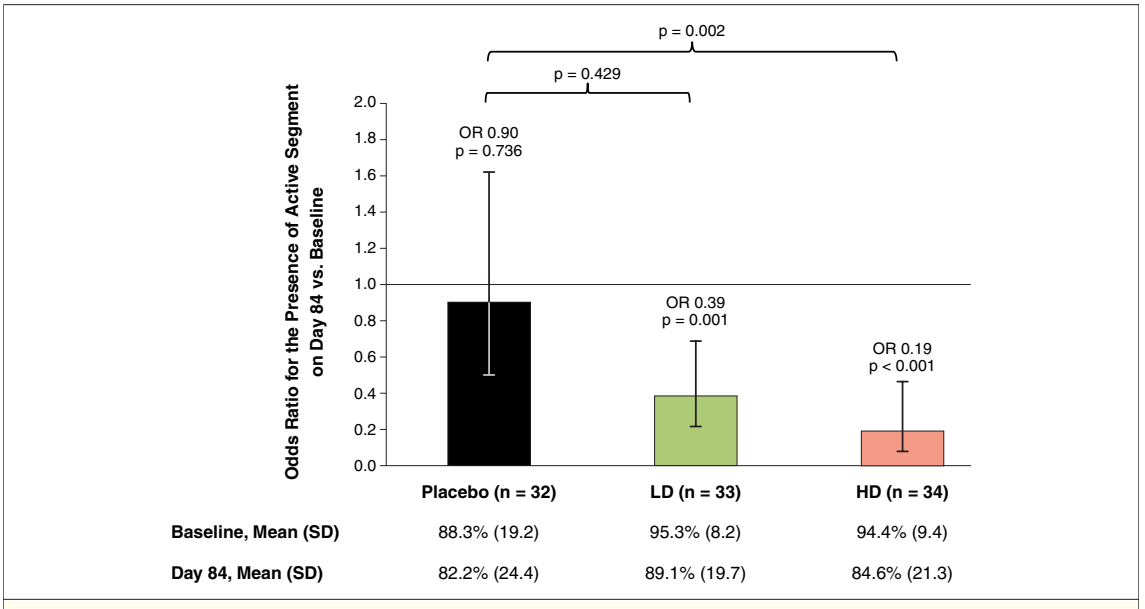

Figure 5. Change in Probability of a Segment Being Active

This figure depicts the odds ratio (OR) and associated 95% confidence intervals for having an inflamed arterial segment (TBR ≥1.6) in the index vessel on day 84 versus baseline in the placebo, losmapimod LD, and losmapimod HD groups. The p values above each **bar** denote the comparison within each group on day 84 compared with baseline (based on logistic regression model with baseline correction within each group); p values above the horizontal parentheses denote the comparison for LD or HD groups versus placebo, after baseline adjustment (based on logistic regression model with both baseline and placebo correction). The numbers underneath the x-axis show the mean (SD) of proportion of active segments at baseline and day 84 for each group. Abbreviations as in Figures 1 and 2.

without significant change in the placebo group (p = 0.736) (Table 2, Fig. 5). After adjusting for baseline and correcting for placebo, the odds of having an active segment on day 84 were significantly lower in the HD group than in the placebo group (p = 0.002), but no significant difference was observed for the LD group versus the placebo group (p = 0.429). This result was maintained irrespective of the TBR cutoff used to define significant inflammation (Online Table 2).

Biomarkers. There was a statistically significant decrease from baseline in average hsCRP over the 84-day treatment period in the HD group compared with the placebo group, and there was a nonsignificant trend for a decrease in the LD group (Table 3, Fig. 6). There was a rebound in hsCRP above baseline levels 2 weeks after cessation of losmapimod treatment (Fig. 6). In the HD group, compared with the placebo group, statistically significant reductions from baseline were also observed at day 84 for interleukin 8, matrix metalloproteinase 9-neutrophil gelatinase associated lipocalin dimer, and monocyte chemotactic protein-1. No reductions were observed for other biomarkers (Table 3).

Visceral and subcutaneous fat imaging. At baseline, there were no significant differences between groups in SUV for FDG for either subcutaneous or visceral fat (Table 4). At day 84, there was a significant reduction from baseline in the HD (but not LD) group in maximum SUV for visceral fat (p = 0.002) that remained statistically significant when compared with placebo (p = 0.018) (Table 4). There were no changes from baseline in maximum SUV for subcutaneous fat in any of the groups. There were no changes in glucose, adiponectin, or insulin levels or body mass index over the course of the study (data not shown).

Safety. Losmapimod was well-tolerated in this study. There were no clinically meaningful changes in laboratory parameters, vital signs, or electrocardiograms over time in any of the groups. Adverse events were reported by a similar proportion of patients in each group (Online Table 3).

DISCUSSION

We conducted an experimental study to assess the effect of a novel anti-inflammatory agent on vascular inflammation, over 3 months, in stable atherosclerotic patients receiving statin therapy. Despite a negative primary endpoint, we demonstrated that losmapimod reduced arterial inflammation, as measured by FDG-PET/CT imaging in the most active discrete segments (pre-defined as a TBR of ≥1.6)

Table 3. Percentage Change From Baseline in Blood Biomarkers

		Day 84 Versus Baseline*			Placebo and Baseline Corrected*		
Biomarker	**Group**	**% Difference**	**95% CI**	**p Value**	**% Difference**	**95% CI**	**p Value**
IL6	HD, n = 34	−21.2	−44.7 to 12.3	0.185	−15.2	−49.3 to 41.9	0.526
	LD, n = 33	12.2	−18.9 to 55.3	0.482	20.8	−26.3 to 98.2	0.450
	Placebo, n = 32	−7.1	−36.0 to 34.9	0.697	NA	NA	NA
IL8	HD, n = 34	−20.9	−33.6 to −5.9	0.009	−26.9	−43.2 to −6.0	0.015
	LD, n = 33	2.1	−13.9 to 21.1	0.813	−5.7	−26.6 to 21.1	0.643
	Placebo, n = 32	8.3	−9.8 to 30.0	0.393	NA	NA	NA
MCP1	HD, n = 34	−8.3	−17.2 to 1.5	0.093	−18.6	−29.9 to −5.5	0.007
	LD, n = 33	0.2	−9.5 to 11.0	0.965	−11.0	−23.3 to 3.4	0.127
	Placebo, n = 32	12.6	0.9 to 25.6	0.034	NA	NA	NA
MMP9	HD, n = 34	−33.4	−45.5 to −18.6	<0.001	−24.7	−43.9 to 1.2	0.060
	LD, n = 33	−19.4	−34.3 to −1.1	0.039	−8.8	−32.3 to 22.8	0.542
	Placebo, n = 32	−11.6	−28.8 to 9.8	0.264	NA	NA	NA
MMP9-NGAL	HD, n = 34	−38.0	−51.0 to −21.5	<0.001	−33.8	−53.3 to −6.4	0.020
	LD, n = 33	−27.7	−43.1 to −8.0	0.009	−22.8	−45.6 to 9.5	0.146
	Placebo, n = 32	−6.2	−27.3 to 21.0	0.619	NA	NA	NA
hsCRP	HD, n = 34	−17.2	−35.7 to 6.5	0.142	−22.0	−46.1 to 12.9	0.187
	LD, n = 33	−1.0	−24.0 to 28.9	0.940	−6.8	−36.1 to 36.1	0.716
	Placebo, n = 32	6.2	−19.0 to 39.2	0.665	NA	NA	NA
hsCRP average†	HD, n = 34	−31.4	−43.9 to −16.2	<0.001	−28.3	−46.1 to −4.5	0.023
	LD, n = 33	−24.0	−38.1 to −6.7	0.009	−20.5	−40.4 to 6.2	0.120
	Placebo, n = 32	−4.4	−22.0 to 17.2	0.664	NA	NA	NA

*Percentage difference, 95% CI, and p value for comparison derived from analysis of covariance. †Average change from baseline over 84-day treatment period.
IL = interleukin; MCP = monocyte chemotactic protein; MMP = matrix metalloproteinase; NGAL = neutrophil gelatinase-associated lipocalin; other abbreviations as in Tables 1 and 2.

of selected arteries, suggesting influence predominantly in the most inflamed areas. Complementing this finding, there was a shift in the distribution of active segments using our frequency analysis. The modest vascular effects were accompanied by significant reductions in circulating inflammatory biomarkers, in line with previous results using this compound (8), and in visceral fat FDG uptake.

A linear correlation in a previous small study between TBR vessel average (which ranged from approximately 1.0 to 4.0) and the tissue level of macrophage marker CD68 (11) drove the decision on our primary endpoint. However, a dearth of segments in our study with baseline TBR substantially >2.0, observed within a narrow range, in addition to the modest effect size, encouraged a more thorough analytic review of the data. FDG-PET/CT imaging is a relatively new, noninvasive method to assess arterial inflammation (26). To date, most interventional FDG-PET/CT studies in cardiovascular patients have been small (14,15) and without clear consensus on the most relevant method of analysis (27). Whereas tests of reproducibility can reasonably employ averaging strategies (20), interventional therapeutic studies often target pre-identified lesions (14,28). We used a variety of methods to examine vascular inflammation across the whole vessel and a more specific focus on active segments of the vascular tree, emulating the evolution of analytic techniques for imaging plaques using coronary intravascular ultrasound (29).

FDG uptake and macrophage activation are closely related in humans (11). The reduction in FDG uptake with therapy in the current study could be due to an attenuation of cellular glucose uptake (30), reduction in macrophage number, or reductions in macrophage hypoxia (12). Although this study cannot determine the precise mechanisms, the original hypothesis for macrophage reduction was based on the correlation between FDG-PET/CT in-vivo and macrophage cell number ex vivo (11).

We also found a significant differential reduction in uptake of FDG in visceral versus subcutaneous adipose tissue following HD losmapimod. FDG-PET imaging of fat to detect its glucose usage is a promising technique in understanding metabolic differences between adipose tissue compartments (31). The fact that this change only occurred in visceral fat implies that there was not a generalized

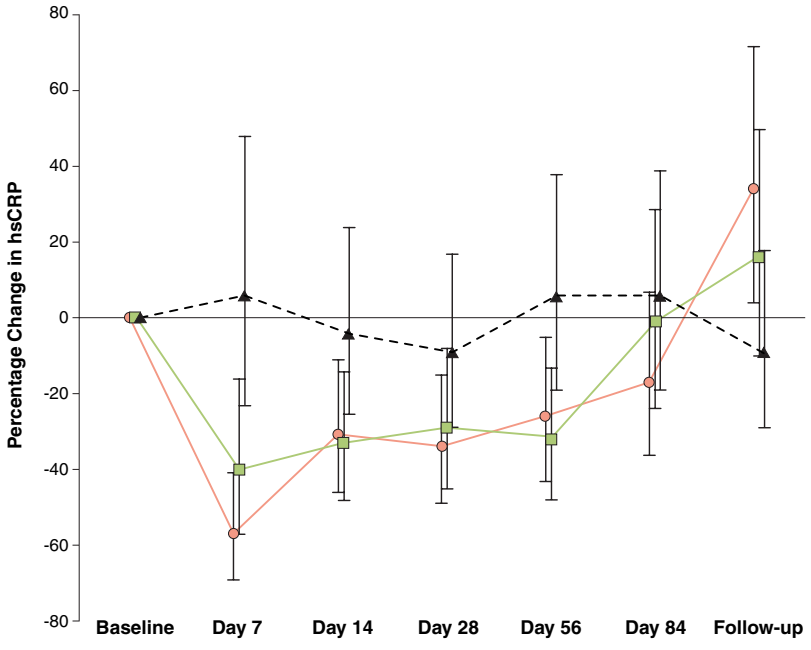

Figure 6. Percentage Change From Baseline in hsCRP

Percentage change from baseline in high-sensitivity C-reactive protein (hsCRP) percentage change (95% confidence intervals) from baseline in hsCRP in the placebo group **(black dashed line)**, losmapimod LD group **(green solid line)**, and losmapimod HD group **(pink solid line)**. Day 7 data includes a subset of the total population (HD: n = 15; LD: n = 13; placebo: n = 14). Abbreviations as in Figure 2.

reduction in FDG uptake in all fat cells. Consistent with this notion, serum glucose levels were not influenced by losmapimod treatment (data not shown). It has previously been shown that visceral fat has a relatively greater FDG uptake than subcutaneous fat does, which was attributed to differential stromal macrophage activity (17). However, adipose cells express p38 MAPK, with glucose uptake thought to be related to tumor necrosis factor alpha expression (a p38 MAPK-mediated cytokine) (32,33). Whereas our findings suggest a selective reduction in macrophage activity with p38 MAPK inhibition, we did not perform adipose tissue biopsies to confirm this hypothesis. In future work, more specific biological imaging agents might help determine whether the effect of losmapimod is due to a reduction in glucose consumption in macrophages or within the adipocytes themselves.

Table 4. Change From Baseline in FDG Uptake in Subcutaneous and Visceral Fat

Change From Baseline in Average Maximum SUV for Subcutaneous Fat								
	Mean ± SD SUV		Day 84 Versus Baseline*			Placebo and Baseline Corrected*		
Group	Baseline	Day 84	Difference	95% CI	p Value	Difference	95% CI	p Value
HD, n = 33	0.32 ± 0.085	0.30 ± 0.095	−0.02	−0.05 to 0.00	0.060	−0.00	−0.04 to 0.03	0.815
LD, n = 32	0.34 ± 0.084	0.31 ± 0.079	−0.03	−0.05 to −0.00	0.020	−0.01	−0.05 to 0.03	0.636
Placebo, n = 30	0.34 ± 0.112	0.32 ± 0.108	−0.02	−0.05 to 0.01	0.168	NA	NA	NA
Change From Baseline in Average Maximum SUV for Visceral Fat								
	Mean ± SD SUV		Day 84 Versus Baseline*			Placebo and Baseline Corrected*		
Group	Baseline	Day 84	Difference	95% CI	p Value	Difference	95% CI	p Value
HD, n = 33	0.59 ± 0.110	0.53 ± 0.120	−0.06	−0.09 to −0.02	0.002	−0.05	−0.09 to −0.01	0.018
LD, n = 32	0.58 ± 0.133	0.56 ± 0.140	−0.02	−0.06 to 0.02	0.274	−0.02	−0.06 to 0.03	0.502
Placebo, n = 30	0.57 ± 0.130	0.57 ± 0.081	−0.01	−0.03 to 0.02	0.654	NA	NA	NA

*Difference, 95% CI, and p value for comparison derived from analysis of covariance.
SUV = standard uptake value; other abbreviations as in Tables 1 and 2.

Study limitations. A limitation of our exploratory study is that a stable patient group was enrolled with well-controlled risk factors, low levels of systemic inflammation, and background statin therapy, likely making any apparent change more difficult to determine. It is possible that the effect would have been greater in patients with higher inflammatory burden. We also excluded patients with chronic disease without active vessel inflammation in whom plaques may be particularly quiescent; therefore, the effect of losmapimod in these especially stable patients is unknown. Finally, we accept the exploratory nature of our approach including the imaging technique and analyses we used to determine vascular effect. The 10% change in FDG-PET/CT observed in a previous statin study (15) suggests that the additional changes reported herein could have clinical relevance.

CONCLUSIONS

In summary, we demonstrate that losmapimod modestly reduced FDG-PET/CT associated vascular inflammation in actively inflamed segments, in conjunction with significant reductions in circulating inflammatory biomarkers as well as FDG uptake in visceral adipose tissue. Inflammation is an important predictor of future cardiovascular events (34,35). We suggest that the role of p38 MAPK inhibition requires further evaluation as a novel therapeutic intervention for atherosclerosis.

Acknowledgments

The authors would like to thank the participating patients, clinical site personnel, Dr. Yasmin for biomarker assays, and Alliance Medical Group for performing the imaging protocols. Editorial assistance was provided by Julie Taylor (funded by GlaxoSmithKline).

Reprint requests and correspondence: Dr. Dennis Sprecher, GlaxoSmithKline, 709 Swedeland Road, UW2421, King of Prussia, Pennsylvania 19406. *E-mail: dennis.l.sprecher@gsk.com.*

REFERENCES

1. Libby P. Inflammation in atherosclerosis. Nature 2002;420:868–74.
2. Senokuchi T, Matsumura T, Sakai M, et al. Extracellular signal-regulated kinase and p38 mitogen-activated protein kinase mediate macrophage proliferation induced by oxidized low-density lipoprotein. Atherosclerosis 2004;176:233–45.
3. Muslin AJ. MAPK signalling in cardiovascular health and disease: molecular mechanisms and therapeutic targets. Clin Sci (Lond) 2008;115:203–18.
4. Seeger FH, Sedding D, Langheinrich AC, Haendeler J, Zeiher AM, Dimmeler S. Inhibition of the p38 MAP kinase in vivo improves number and functional activity of vasculogenic cells and reduces atherosclerotic disease progression. Basic Res Cardiol 2010;105:389–97.
5. Willette RN, Eybye ME, Olzinski AR, et al. Differential effects of p38 mitogen-activated protein kinase and cyclooxygenase 2 inhibitors in a model of cardiovascular disease. J Pharmacol Exp Ther 2009;330:964–70.
6. Morris JB, Olzinski AR, Bernard RE, et al. p38 MAPK inhibition reduces aortic ultrasmall superparamagnetic iron oxide uptake in a mouse model of atherosclerosis: MRI assessment. Arterioscler Thromb Vasc Biol 2008;28:265–71.
7. Sarov-Blat L, Morgan JM, Fernandez P, et al. Inhibition of p38 mitogen-activated protein kinase reduces inflammation after coronary vascular injury in humans. Arterioscler Thromb Vasc Biol 2010;30:2256–63.
8. Cheriyan J, Webb AJ, Sarov-Blat L, et al. Inhibition of p38 mitogen-activated protein kinase improves nitric oxide-mediated vasodilatation and reduces inflammation in hypercholesterolemia. Circulation 2011;123:515–23.
9. Kubota R, Yamada S, Kubota K, Ishiwata K, Tamahashi N, Ido T. Intratumoral distribution of fluorine-18-fluorodeoxyglucose in vivo: high accumulation in macrophages and granulation tissues studied by microautoradiography. J Nucl Med 1992;33:1972–80.
10. Ogawa M, Magata Y, Kato T, et al. Application of 18F-FDG PET for monitoring the therapeutic effect of antiinflammatory drugs on stabilization of vulnerable atherosclerotic plaques. J Nucl Med 2006;47:1845–50.
11. Tawakol A, Migrino RQ, Bashian GG, et al. In vivo 18F-fluorodeoxyglucose positron emission tomography imaging provides a noninvasive measure of carotid plaque inflammation in patients. J Am Coll Cardiol 2006;48:1818–24.
12. Folco EJ, Sheikine Y, Rocha VZ, et al. Hypoxia but not inflammation augments glucose uptake in human macrophages implications for imaging atherosclerosis with 18fluorine-labeled 2-deoxy-D-glucose positron emission tomography. J Am Coll Cardiol 2011;58:603–14.
13. Rudd JH, Warburton EA, Fryer TD, et al. Imaging atherosclerotic plaque inflammation with [18F]-fluorodeoxyglucose positron emission tomography. Circulation 2002;105:2708–11.
14. Tahara N, Kai H, Ishibashi M, Nakaura H, et al. Simvastatin attenuates plaque inflammation: evaluation by fluorodeoxyglucose positron emission tomography. J Am Coll Cardiol 2006;48:1825–31.
15. Lee SJ, On YK, Lee EJ, Choi JY, Kim BT, Lee KH. Reversal of vascular 18F-FDG uptake with plasma high-density lipoprotein elevation by atherogenic risk reduction. J Nucl Med 2008;49:1277–82.
16. Tahara N, Kai H, Yamagishi S, et al. Vascular inflammation evaluated by [18F]-fluorodeoxyglucose positron emission tomography is associated with the metabolic syndrome. J Am Coll Cardiol 2007;49:1533–9.
17. Rosito GA, Massaro JM, Hoffmann U, et al. Pericardial fat, visceral abdominal fat, cardiovascular disease risk factors, and vascular calcification in a community-based sample: the Framingham Heart Study. Circulation 2008;117:605–13.

18. Christen T, Sheikine Y, Rocha VZ, et al. Increased glucose uptake in visceral versus subcutaneous adipose tissue revealed by PET imaging. J Am Coll Cardiol Img 2010;3:843–51.
19. Rudd JH, Myers KS, Bansilal S, et al. Atherosclerosis inflammation imaging with 18F-FDG PET: carotid, iliac, and femoral uptake reproducibility, quantification methods, and recommendations. J Nucl Med 2008;49:871–8.
20. Rudd JH, Myers KS, Bansilal S, et al. (18)Fluorodeoxyglucose positron emission tomography imaging of atherosclerotic plaque inflammation is highly reproducible: implications for atherosclerosis therapy trials. J Am Coll Cardiol 2007;50:892–6.
21. Fayad ZA, Mani V, Woodward M, et al. Rationale and design of dal-PLAQUE: A study assessing efficacy and safety of dalcetrapib on progression or regression of atherosclerosis using magnetic resonance imaging and 18F-fluorodeoxyglucose positron emission tomography/computed tomography. Am Heart J 2011;162:214–21.e2.
22. Graebe M, Pedersen SF, Højgaard L, Kjaer A, Sillesen H. 18FDG PET and ultrasound echolucency in carotid artery plaques. J Am Coll Cardiol Img 2010;3:289–95.
23. Pedersen SF, Graebe M, Fisker Hag AM, Højgaard L, Sillesen H, Kjaer A. Gene expression and 18FDG uptake in atherosclerotic carotid plaques. Nucl Med Commun 2010;31:423–9.
24. Martin-Ventura JL, Blanco-Colio LM, Gomez-Hernandez A, et al. Intensive treatment with atorvastatin reduces inflammation in mononuclear cells and human atherosclerotic lesions in one month. Stroke 2005;36:1796–800.
25. Ribeiro-Filho FF, Faria AN, Azjen S, Zanella MT, Ferreira SR. Methods of estimation of visceral fat: advantages of ultrasonography. Obes Res 2003;11:1488–94.
26. Sheikine Y, Akram K. FDG-PET imaging of atherosclerosis: do we know what we see? Atherosclerosis 2010;211:371–80.
27. Menezes LJ, Kotze CW, Hutton BF, et al. Vascular inflammation imaging with 18F-FDG PET/CT: when to image? J Nucl Med 2009;50:854–7.
28. Lee JM, Wiesmann F, Shirodaria C, et al. Early changes in arterial structure and function following statin initiation: quantification by magnetic resonance imaging. Atherosclerosis 2008;197:951–8.
29. Nissen SE, Nicholls SJ, Sipahi I, et al., for the ASTERIOD Investigators. Effect of very high-intensity statin therapy on regression of coronary atherosclerosis: the ASTEROID trial. J Am Med Assoc 2006;295:1556–65.
30. Deichen JT, Prante O, Gack M, Schmiedehausen K, Kuwert T. Uptake of [18F]fluorodeoxyglucose in human monocyte-macrophages in vitro. Eur J Nucl Med Mol Imaging 2003;30:267–73.
31. Gropler RJ, Peterson LR. Adipose tissue imaging the potential and the challenge. J Am Coll Cardiol Img 2010;3:852–3.
32. Sweeney G, Somwar R, Ramlal T, Volchuk A, Ueyama A, Klip A. An inhibitor of p38 mitogen-activated protein kinase prevents insulin-stimulated glucose transport but not glucose transporter translocation in 3T3-L1 adipocytes and L6 myotubes. J Biol Chem 1999;274:10071–8.
33. Hauner H, Petruschke T, Russ M, Röhrig K, Eckel J. Effects of tumour necrosis factor alpha (TNF alpha) on glucose transport and lipid metabolism of newly-differentiated human fat cells in cell culture. Diabetologia 1995;38:764–71.
34. Wilson PW, Pencina M, Jacques P, Selhub J, D'Agostino R Sr., O'Donnell CJ. C-reactive protein and reclassification of cardiovascular risk in the Framingham Heart Study. Circ Cardiovasc Qual Outcomes 2008;1:92–7.
35. Ridker PM. Clinical application of C-reactive protein for cardiovascular disease detection and prevention. Circulation 2003;107:363–9.

Key Words: atherosclerosis ■ biomarkers ■ imaging ■ inflammation ■ p38 mitogen-activated protein kinase inhibition ■ randomized controlled trial.

▶ APPENDIX

For supplementary methods and tables, please see the online version of this paper.